atmosphere

MDPI

Article

Downscaling Atmosphere-Ocean Global Climate Model Precipitation Simulations over Africa Using Bias-Corrected Lateral and Lower Boundary Conditions

Leonard M. Druyan [1,2,*] and Matthew Fulakeza [1,3]

[1] NASA/Goddard Institute for Space Studies, New York, NY 10025, USA; mfulakeza@gmail.com
[2] Dept. of Applied Physics and Math, Columbia University, New York, NY 10025, USA
[3] Center for Climate Systems Research, Columbia University, New York, NY 10025, USA
* Correspondence: leonard.m.druyan@nasa.gov

Received: 4 September 2018; Accepted: 29 November 2018; Published: 12 December 2018

Abstract: A prequel study showed that dynamic downscaling using a regional climate model (RCM) over Africa improved the Goddard Institute for Space Studies Atmosphere-Ocean Global Climate Model (GISS AOGCM: ModelE) simulation of June–September rainfall patterns over Africa. The current study applies bias corrections to the lateral and lower boundary data from the AOGCM driving the RCM, based on the comparison of a 30-year simulation to the actual climate. The analysis examines the horizontal pattern of June–September total accumulated precipitation, the time versus latitude evolution of zonal mean West Africa (WA) precipitation (showing monsoon onset timing), and the latitude versus altitude cross-section of zonal winds over WA (showing the African Easterly Jet and the Tropical Easterly Jet). The study shows that correcting for excessively warm AOGCM Atlantic sea-surface temperatures (SSTs) improves the simulation of key features, whereas applying 30-year mean bias corrections to atmospheric variables driving the RCM at the lateral boundaries does not improve the RCM simulations. We suggest that AOGCM climate projections for Africa should benefit from downscaling by nesting an RCM that has demonstrated skill in simulating African climate, driven with bias-corrected SST.

Keywords: regional climate models; dynamic downscaling AOGCM simulations; West African monsoon onset

1. Introduction

1.1. Characteristics of the West African (WA) Monsoon System

Thorncroft et al. (2011) [1] organized the annual cycle of the WA(West Africa) climate according to the following major stages, based on an analysis of European Centre for Medium-Range Weather Forecasts Interim reanalysis (ERA-I) data, 1989–2009: (1) An "oceanic" phase from November to mid-April, featuring a broad rain band with peak values just north of the Equator; (2) a "coastal" phase from mid-April to the end of June, featuring a rainfall peak in the coastal region around 4° N (over the ocean); (3) a transitional "break" phase during early July, when WA rainfall is at a minimum; and (4) a Sahelian phase between mid-July and September, when a more intense rainfall peak is established in the Sahel region around 10° N. This organization is consistent with Gu and Adler (2004) [2], who also described the break in West African rainfall during phase 3.

Mohino et al. (2011) [3] studied the relationship between Sahel rainfall and sea-surface temperature (SST) decadal variability. Based on their global climate model (GCM) experiments,

they concluded that the low-frequency variability of Sahel rainfall reflects a competition of three modes of SST variability. Accordingly, Sahel precipitation is statistically linked to (1) the long-term warming trend of global SSTs (global warming is GW), which is influenced by natural and anthropogenic forcing; (2) the Atlantic Multidecadal Oscillation (AMO); and (3) the Interdecadal Pacific Oscillation (IPO). Droughts are favored during negative phases of the AMO (cool Atlantic SST) and positive phases of the IPO (warm Pacific SST). For example, the three SST conditions unfavorable for Sahel precipitation coincided during the 1980s drought: A positive GW trend, a negative phase of the AMO, and a positive phase of the IPO. In addition, other studies by Jung et al. (2006) and Rowell (2003) [4,5] have suggested that positive SST anomalies in the Mediterranean can contribute to positive Sahel rainfall anomalies. Druyan (2011) and Nicholson (2013) [6,7] have reviewed other studies that discussed SST influences on Sahel precipitation trends.

The combined influences of increased concentrations of greenhouse gases, land surface changes, and evolving SST anomalies on WA rainfall trends and on the various components of the WA monsoon need to be researched with models that have demonstrated skill in simulating the WA climate. Consensus from many modeling systems and a convincing process analysis to explain results will increase confidence in conclusions. Druyan and Fulakeza (2016) [8] documented Goddard Institute for Space Studies Atmosphere-Ocean Global Climate Model (GISS AOGCM) ModelE SST biases of 4–8C for June-September (JJAS) 1998–2002 in the southeast Atlantic Ocean. Given the aforementioned sensitivity of WA summer climate to SST, evaluating the impact of bias corrections on the lower boundary conditions is a promising avenue of research.

1.2. Dynamic Downscaling with Regional Models: Simulating the African Summer Monsoon Climate

Regional climate models (RCMs) can improve the spatial representation of climate features by downscaling coarse grid global analyses or decadal climate extrapolations to higher resolutions. Lateral and lower boundary conditions (LBCs and SSTs) from global data sets provide the RCMs with global connectivity. Lim et al. (2011) [9] found that downscaling the National Center for Environmental Prediction reanalysis 2 (NCPR2) (Kanamitsu et al. 2002, [10]) with an RCM to a 20-km computational grid simulated a mean summertime precipitation distribution with better spatial detail (as validated by observations) than the NCPR2 precipitation did. Denis et al. (2002) [11] documented the advantages of RCM downscaling to a 45-km grid, assessing RCM improvements in spatial and temporal variability compared to the forcing data. Their one-way nesting strategy skillfully downscaled large-scale information to the regional scales. They additionally showed that the temporal means and variability of several observed fine-scale climate parameters were effectively reproduced, particularly where mesoscale surface forcings were strong. Improvements over the ocean and away from the surface are less striking. Haensler et al. (2011) [12] investigated the skill of the REMO RCM in simulating mesoscale climate patterns. Their methodology incorporated double-nesting, with an inner grid spacing of about 18 km. Their outermost lateral boundary forcing was the European Centre for Medium-Range Weather Forecasts 40-year reanalysis (ERA40). They found that the RCM results validated well against the spatial and temporal variability of climate observations. The added value of the RCM product was recognized, compared to the forcing ERA40 data, achieving a significantly better representation of seasonal rainfall amounts.

There is great interest in improving the assessments of climate change for Africa. The Intergovernmental Panel on Climate Change (IPCC) 4th Assessment Report (Bernstein et al. 2007) [13] emphasized that "Africa is one of the most vulnerable continents because of the range of projected impacts, multiple stresses and low adaptive capacity." On the other hand, there is no consensus among IPCC 4th Assessment climate change prediction models about how water availability in West Africa will change toward the end of the 21st century (Druyan 2011) [6]. The sustainability of many African regions is acutely sensitive to climate, so reliable projections of climate trends could contribute to overcoming negative impacts.

RCM experiments can test the relative merits of alternative sets of LBCs and SSTs, estimating the sensitivity of the RCM product to alternative forcing analyses. Druyan and Fulakeza (2013) [14] found that the NCPR2 LBCs during 1998–2002 produced a weaker WA monsoon circulation and lower rainfall accumulations than the ERA-I LBCs did. Diallo et al. (2012) [15] recommend using multiple GCM and RCM ensembles to improve the reference simulations of rainfall and temperature over West Africa and to create consistent climate change scenarios. Their study was based on a set of four different RCMs driven by two GCMs simulating the IPCC A1B scenario to assess mid-21st century climate over WA. Most of those models predicted a significant decrease in rainfall near the western African coast and over the western Sahel, associated with stronger warming found there. However, they reported less consensus regarding climate projections southward and eastward, and therefore less confidence in those projections. Patricola and Cook (2010) [16] projected a mosaic of drought and rainy months for the late 21st century based on WRF simulations driven by climate change signals from nine AOGCM runs. Vigaud et al. (2011) [17] analyzed WRF climate changes over West Africa between the 1980s and the 2030s by downscaling ARPEGE-CLIMAT GCM output. Their WRF simulation forced by ERA40 1980s boundary conditions produced a July–September mean precipitation distribution that was spatially reasonable, but with exaggerated orographic maxima. Corresponding simulations forced by ARPEGE produced more moderate means, but missed important orographic maxima over the highlands of Guinea and Cameroon. Consequently, their WRF A2 scenario climate changes are difficult to interpret. Contrary to Diallo et al. (2012) [15], results from Vigaud et al. (2011) [17] did not show any significant decreases in Sahel precipitation for the 2030s, but rather substantial rainfall increases over the Gulf of Guinea and the eastern Sahel. The enhancement related to higher evaporation that in turn led to increased moisture advection toward eastern regions of the Gulf of Guinea. They also suggested that future warmer conditions over both the Mediterranean region and the northeastern Sahel may also participate in enhancing moisture transport within the African Easterly Jet (AEJ). Unrealistic features in their 1980s simulations made their projections suspect.

Paeth and Thamm (2007) [18] reported on the impacts of greenhouse warming and land degradation on African precipitation. Their study used REMO RCM simulations on a 0.5° grid, forced by ECHAM4/HOPE global model projections (according to the IPCC B2 scenario) up to 2025. Paeth and Thamm (2007) [18] found that future strengthening of the WA summer monsoon circulation from enhanced continental surface heating was more than offset by inhibited evapotranspiration due to reduced vegetation and soil degradation. Lower evapotranspiration, in turn, reduced modeled moist convection, favoring drought in the Sahel. In a related finding, Steiner et al (2009) [19] showed that RCM simulations of the WA summer monsoon were sensitive to the model's land surface and hydrology scheme. Thus, coupling of the Community Land Model (CLM3) to the RegCM3 RCM markedly improved the simulation of the WA mean climate relative to a previous version of RegCM3 coupled to the Biosphere Atmosphere Transfer Scheme (BATS). Based on two 10-year simulations (1992–2001), the seasonal timing and mean monsoon precipitation rates more closely matched observations when the new land surface scheme was implemented. Accordingly, RegCM3–CLM3 improved the timing of the monsoon advance and retreat across the Guinean Coast, and lessened a positive precipitation bias in the Sahel and Northern Africa. However, a regional modeling study by Moufouma-Okia and Rowell (2010) [20] found that WA summer monsoon precipitation was not sensitive to initial soil moisture specification prescribed for the spring, although they cautioned that these results may have been model-dependent. Any impacts of initial soil moisture were presumably minimized by LBCs that imported moisture into the region. Alo and Wang (2010) [21] described a regional model study that demonstrated the considerable influence of natural land vegetation structure on the decadal evolution of Sahel rainfall. Giannini et al. (2013) [22] proposed that the differential warming of the subtropical North Atlantic, outpacing warming of the global tropical oceans, will provide enough excess moisture to make the Sahel wetter in the 21st century than during the 1970s and 1980s.

Sylla et al. (2010) [23] analyzed the skill of a recent version of the RegCM3 RCM in reproducing seasonal mean climatologies, annual cycle, and interannual climate variability over continental Africa

and several climate subregions. The ERA-I (0.75° grid) was used to provide initial and LBCs for the continuous 17-year integration over Africa, from January 1989 to December 2005. The RCM was integrated on a horizontal grid of 50 km. The mean annual cycle of precipitation was realistically simulated, including single and multiple rainy seasons, as was the observed interannual variability of precipitation over most of the African subregions. In some cases, the RCM even improved the configuration of derived ERA-I precipitation. In addition, Sylla et al. (2011) [24] investigated the sensitivity of the WA summer monsoon climate to the inclusion or exclusion of deep convection in two 5-year simulations with the RegCM3.

The Coordinated Regional Downscaling Experiment (CORDEX) downscaled AOGCM prognostics of decadal climate change (Jones et al. 2011) [25] using RCMs. Africa was a CORDEX priority region. RCM performances in simulating the contemporary climate based on forcing from ERA-I (0.75° grid) from 1989–2008 were given by Druyan and Fulakeza (2013), Hernandez-Diaz et al. (2012) and Nikulin et al. (2012) [14,26,27]. Adeniyi and Dilau (2018) [28] used CORDEX RCMs for a recent assessment of the link between WA drought and Atlantic SST anomalies. The current study employs the RCM grid spacing of 0.44° (about 49 km) used in the CORDEX studies.

This paper aims to contribute to the goal of improved climate change projections for West Africa (WA) by applying bias corrections to the boundary conditions of a regional climate model. The reliability of climate change projections is reflected in a model's skill in simulating observable contemporary climate variability. This study, therefore, examines the impact of bias corrections on simulations for a historical period (1998–2002) to test the concept.

1.3. Bias Corrections

Druyan and Fulakeza (2016) [8] showed that several AOGCM-simulated climate features of the West African summer monsoon system based on 2° by 2.5° horizontal resolution were made more realistic by downscaling with the RM3 to a 0.44° latitude by longitude grid. However, RCM simulations, driven by global model simulations, can be contaminated by unrealistic data from the driving model (Misra and Kanamitsu 2004, Rojas and Seth 2003;) [29,30]. Thus, systematic climate biases in the AOGCM forcing can eventually cause biases in the downscaled climate. There have been attempts to mitigate such biases. Misra and Kanamitsu (2004) [29] applied bias corrections in simulating historical seasonal climate simulations. Aryal and Zhu (2017) [31] used bias correction techniques to investigate how they affected the statistics of regional climate model-simulated drought frequency and severity. However, their study applied bias corrections to simulated precipitation in contrast to the present effort that corrects biases in the LBCs and SSTs driving the RCM. In particular, bias correction of LBCs and SSTs is adapted here to investigate the impact on 1998–2002 simulated means. Bias corrections are calculated that force 30-year mean AOGCM-simulated climate variables over an historical period (1979–2008) to agree with observations-based reanalysis, in this case ERA-I. The study assesses the benefits of applying these bias corrections for the regional model simulation of the 5-year period. Finally, we suggest that the bias correction approach could be applied to AOGCM projections of decadal climate change, although that research could not be completed for this paper.

2. Models and Data

2.1. The GISS Atmosphere-Ocean Global Climate Model

This study uses data from the 1979–2008 simulation of a CMIP5 version of GISS ModelE2-R (with "Russell ocean") (hereafter ModelE) (Miller et al., 2014; Schmidt et al., 2006; Schmidt et al., 2014) [32–34]. ModelE is optimized to simulate realistic climate variability globally, but not specifically for Africa. Downscaling experiments here span the interval November 1997 to October 2002. AOGCM data are computed and saved on a horizontal grid 2.0° latitude by 2.5° longitude, globally at 40 vertical layers. The hydrostatic approximation is incorporated by using pressure as a vertical coordinate, with terrain-following sigma coordinates in the 23 layers below 150 hPa. Above 150 hPa, layer thicknesses

were horizontally uniform to the model top at 0.1 hPa. Vertical resolution is increased near the lower boundary, with six layers below 825 hPa, whereas there are nine layers between 251 and 43 hPa. ModelE2 relies on a mass flux cumulus parameterization described by Del Genio and Yao (1993) [35], which includes a cloud base neutral buoyancy flux closure with two entraining plumes sharing the mass flux. Stratiform clouds were computed by a Sundqvist-type prognostic cloud water technique with diagnostic cloud fractions (Del Genio et al., 1996) [36]. The cloud liquid water scheme simulates life cycle effects in stratiform clouds and allows cloud optical properties to be determined interactively. The land surface model computes the relative contributions of transpiration and soil evaporation for vegetated areas, as in Schmidt et al. (2006) [33]. There are nine vegetation cover categories with some improvements to the soil biophysics and vegetation components based on the Ent Terrestrial Biosphere Model (Kim et al. 2015) [37]. The land surface model consists of two integrated parts, the soil and the canopy, and it conserved water and heat while simulating their vertical fluxes. The modeled soil is divided into six layers to a depth of 3.5 m, and it discriminates between five different soil types. The canopy, modeled as a separate layer located above the soil, computes the interception of precipitation, evaporation of accumulated water, and evaporation of soil water.

In this study, ModelE simulations deliver time-dependent LBCs and SSTs to drive the regional climate model, RM3. ModelE output is from a single realization, and the current study uses these data to form LBCs and SSTs 4 times per day (6 h intervals).

Validation of simulation results is made against Tropical Rainfall Measuring Mission (TRMM) (Huffman et al. 2007, [38]) satellite-based precipitation rate estimates.

2.2. Regional Climate Model, Version 3 (RM3)

The RM3 has been advantageously applied to previous studies of climate variability over Africa (Druyan et al., 2006, 2008, 2010; Druyan and Fulakeza, 2013) [14,39–41]. The RM3 structure shares with ModelE the Del Genio and Yao (1993) [35] moist convection parameterization and the Del Genio et al. (1996) [36] scheme for the effects of cloud liquid water. The RM3 ground hydrology scheme was adapted from the then-corresponding GISS GCM model component in 2002. The RM3 ground hydrology scheme for the current experiments is therefore similar to the corresponding ModelE scheme, but the algorithms for the interception of precipitation water by the canopy and for the surface runoff in ModelE, and not RM3, have since been modified according to the Ent Terrestrial Biosphere Model (Kim et al. 2015) [37]. Surface evapotranspiration can therefore evolve differently in the two models.

3. Simulation Experiments: Computation of Bias Corrections

We adapt the "anomaly nesting" approach of Misra and Kanamitsu (2004) [29], intended to mitigate unfavorable effects of AOGCM (ModelE) biases on LBCs and SSTs. Misra and Kanamitsu (2004) [29] applied the methodology to contemporary seasonal climate simulations, and we adapt it to modify 1998–2002 simulations over Africa. The procedure begins with the computation of the 30-year (1979–2008) mean annual cycle of each variable (SST, temperature, u wind, v wind, relative humidity, and geopotential height) computed 4 times per day at each grid element from the ModelE simulation. The parallel 30-year mean annual cycles of the same variables are also extracted from ERA-I data for the same period. An annual cycle of ModelE biases is computed 4 times per day by subtracting the ERA-I 30-year climatology from the ModelE 30-year climatology. This study assumes that correcting for the AOGCM's historical systematic biases eliminates many unrealistic features of the AOGCM climatology that may have contaminated the LBCs and SSTs. The weakness of the approach for eventual estimates of decadal climate change is that AOGCM climate biases (relative to observations) may evolve throughout the 21st century in a way not accommodated by the bias corrections.

The AOGCM biases are subtracted from each variable 4 times per day to form all LBCs and SSTs for driving the RM3 during 1998–2002. (In effect, adjusted AOGCM variables are AOGCM departures from model climatology added to ERA-I climatology.) RM3 simulations are forced by the adjusted LBCs and SSTs for the 5-year historical period 1998–2002. We also evaluate simulations with only SST

bias corrections. Impacts of climate change would be taken as the differences between RM3 simulations forced by the adjusted boundary conditions for a selected future period relative to the RM3 results for this base period. Patricola and Cook (2010) [16] mitigated AOGCM biases in LBCs by adding AOGCM climate change signals to a 20-year reanalysis climatology. The current alternative approach retaines synoptic variability in the LBCs, which may include incipient African easterly waves (AEWs). The RM3 simulations using uncorrected boundary conditions are hereafter referred to as "RM3nc". The runs driven by bias-corrected LBCs and SSTs are hereafter referred to as RM3bc, and the runs based on only SST corrections as RM3sst.

4. Results

4.1. JJAS Precipitation Accumulations

Figure 1a shows the JJAS 1998–2002 mean precipitation accumulation observed by TRMM (Tropical Rainfall Measuring Mission) (Huffman et al. 2007) [38], and Figure 1b shows the corresponding distribution of RM3nc precipitation forced by uncorrected ModelE LBCs and SST, which was previously shown to be a big improvement over the ModelE results (Druyan and Fulakeza 2016) [8]. Figure 1c shows results from the RM3 simulated with bias-corrected ModelE LBCs and SST (RM3bc). The ITCZ in Figure 1c is more realistically narrower, and the maxima of the WA rain band are more realistically less extreme, compared to the simulations forced by uncorrected LBCs. Figure 1d shows the results of correcting SST biases and not LBCs (RM3sst). The ITCZ maximum near the western boundary is less realistic, but lower accumulations over West Africa represent an improvement. The orographic maximum at the Atlantic (Guinea) coast is appropriately simulated by RM3nc (Figure 1b), whereas the maximum is similar for both RM3bc and RM3sst.

Figure 2a shows JJAS 1998–2002 precipitation accumulation errors (against TRMM) for RM3nc using ModelE uncorrected LBCs and SST. Monsoon rainfall over West Africa is exaggerated by some 300–800 mm. Errors over the equatorial Atlantic also exceeded 300 mm. Figure 2b shows the corresponding (JJAS 1998–2002 precipitation accumulation) errors (against TRMM) for RM3bc, driven by ModelE LBC and SST with bias corrections. Bias-corrected LBCs and SST are shown to have considerably reduced positive WA monsoonal precipitation errors as well as excesses along the Equator. Figure 2c shows the departures from TRMM for the results with only bias-corrected SST (RM3sst, Figure 1d). Over WA, errors range between 0 and 300 mm, replacing errors exceeding 300 mm in Figure 2b. Large negative errors over the eastern ITCZ in Figure 2b are mitigated. Druyan and Fulakeza (2016) [8] showed that uncorrected ModelE SST forcing contained a strong positive bias in the eastern South Atlantic and the Gulf of Guinea. The excess monsoon precipitation over WA in Figure 2a is consistent with positive SST anomalies in the Gulf of Guinea (Druyan and Fulakeza, 2014) [42]. Previously, Druyan and Fulakeza (2016) [8] found that substituting observed SST in place of ModelE-computed SST reduced downscaled seasonal precipitation errors over WA.

This explains the aforementioned impacts of SST bias corrections on the downscaling results. This analysis of Figures 1 and 2 suggests that little to no advantage to the simulated seasonal precipitation field is gained by driving RM3 with-bias corrected LBCs, whereas big improvements are achieved by correcting SST biases.

4.2. Pentad (5-Day Mean) Precipitation versus Latitude over WA

Figure 3 shows the seasonal march of pentad (5-day mean) precipitation rates versus latitude over WA (10° W to 10° E) between 1–5 June (pentad 1) and 24–28 September (pentad 24) for TRMM data and each of the three simulations, averaged over 1998–2002. ModelE simulated a rather stationary WA rain band along 8° N, June–September (see Druyan and Fulakeza 2016, [8]). As such, ModelE simulations did not represent the observed latitudinal jump of the rain band (TRMM, Figure 3a) that signaled "onset", usually in early July. Downscaling ModelE simulations with RM3nc improves the modeled onset (Figure 3b), but its transition is more gradual than the observed. Figure 3c shows that

RM3bc does not improve the configuration of this northward thrust, although it does better represent the midsummer precipitation maximum over the Sahel (along 10° N). Figure 3d, however, shows that the RM3sst simulations using only SST bias corrections nicely captures the observed jump of the rain band from 5° N to 10° N at pentad 8 (6–10 July).

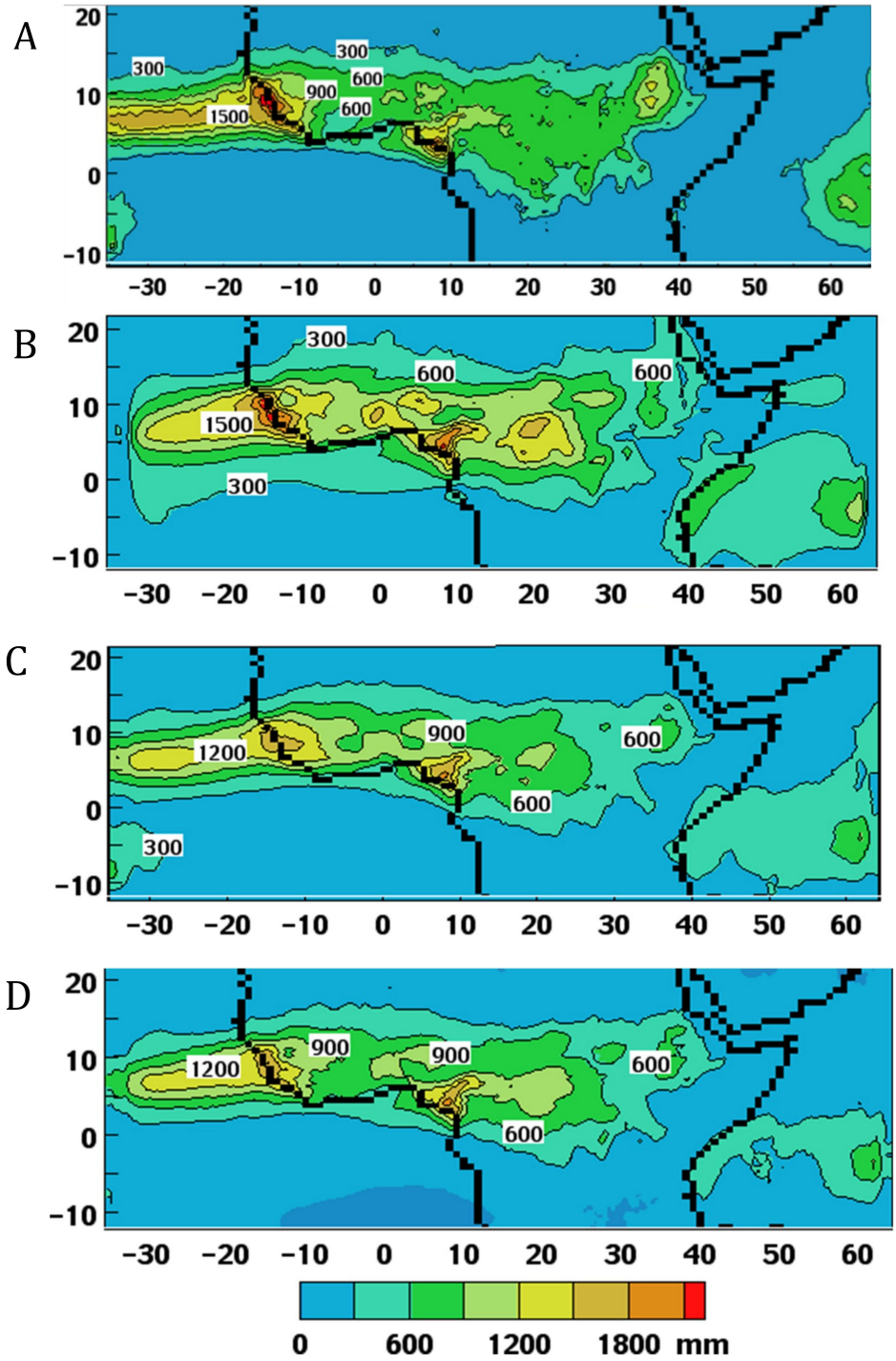

Figure 1. June–September precipitation accumulations (mm), averaged over 1998–2002: (**A**) Tropical Rainfall Measuring Mission (TRMM); (**B**) RM3nc forced by ModelE without bias corrections; (**C**) RM3bc forced by ModelE with bias corrections to LBCs and sea-surface temperature (SST); (**D**) RM3sst forced by ModelE with bias corrections to only SST.

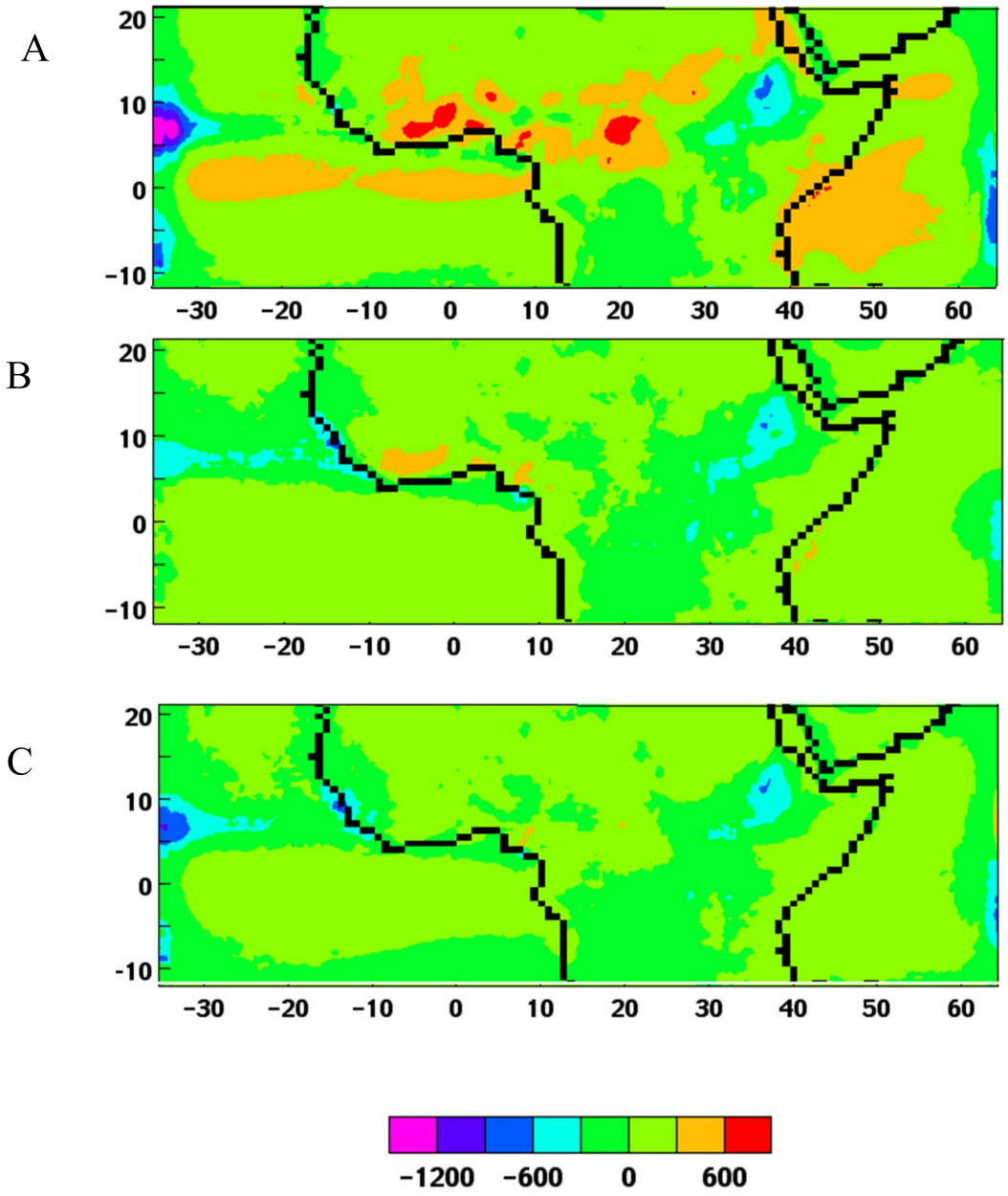

Figure 2. Errors in simulated June–September 1998–2002 precipitation accumulations (mm). (**A**) RM3nc forced by ModelE without bias corrections; (**B**) RM3bc forced by ModelE with bias corrections to LBCs and SST; (**C**) RM3sst forced by ModelE with bias corrections to only SST.

4.3. JJAS Mean Zonal Circulation for WA

Figure 4 shows latitude-pressure (height) cross-sections of zonal winds averaged over JJAS 1998–2002 and averaged over the longitudinal range of 10° W to 10° E. The major features depicted by ERA-I circulation data (Figure 4a) are the Tropical Easterly Jet (TEJ) at 6° N, 200 hPa; the African easterly jet (AEJ) at 12° N, 600 hPa; monsoon westerlies below 800 hPa; and Harmattan near-surface easterlies north of 20° N. The TEJ is associated with upper tropospheric divergence that deepens cyclones and enhances deep convection, whereas the AEJ provides energy to grow African easterly waves, which are precursors to Atlantic tropical cyclones. Accordingly, unrealistic simulations of these jet streams may have contributed to model errors of salient WA climate features. ModelE simulations failed to represent the TEJ over WA during JJAS, and ModelE AEJ core speeds were slightly too strong (see Druyan and Fulakeza 2016) [8]. It was previously shown that downscaling with RM3nc

(Figure 4b) improved both TEJ and AEJ core speeds (against ERA-I). Figure 4c shows the corresponding cross-section for the RM3bc simulations with bias corrections to the LBCs and SST. Results show that the bias corrections additionally improve the core speeds of the TEJ and the AEJ by speeding up the TEJ and slowing the AEJ. Moreover, the bias corrections mitigate some of the excessive vertical shear above 0–5° N. Figure 4d shows the zonal wind cross-section for the RM3sst simulations using only SST bias corrections. Here the TEJ is even stronger, as are the near-surface westerlies, both giving better agreement with ERA-I. The AEJ in Figure 4d is somewhat stronger, but not less realistic than in the other panels.

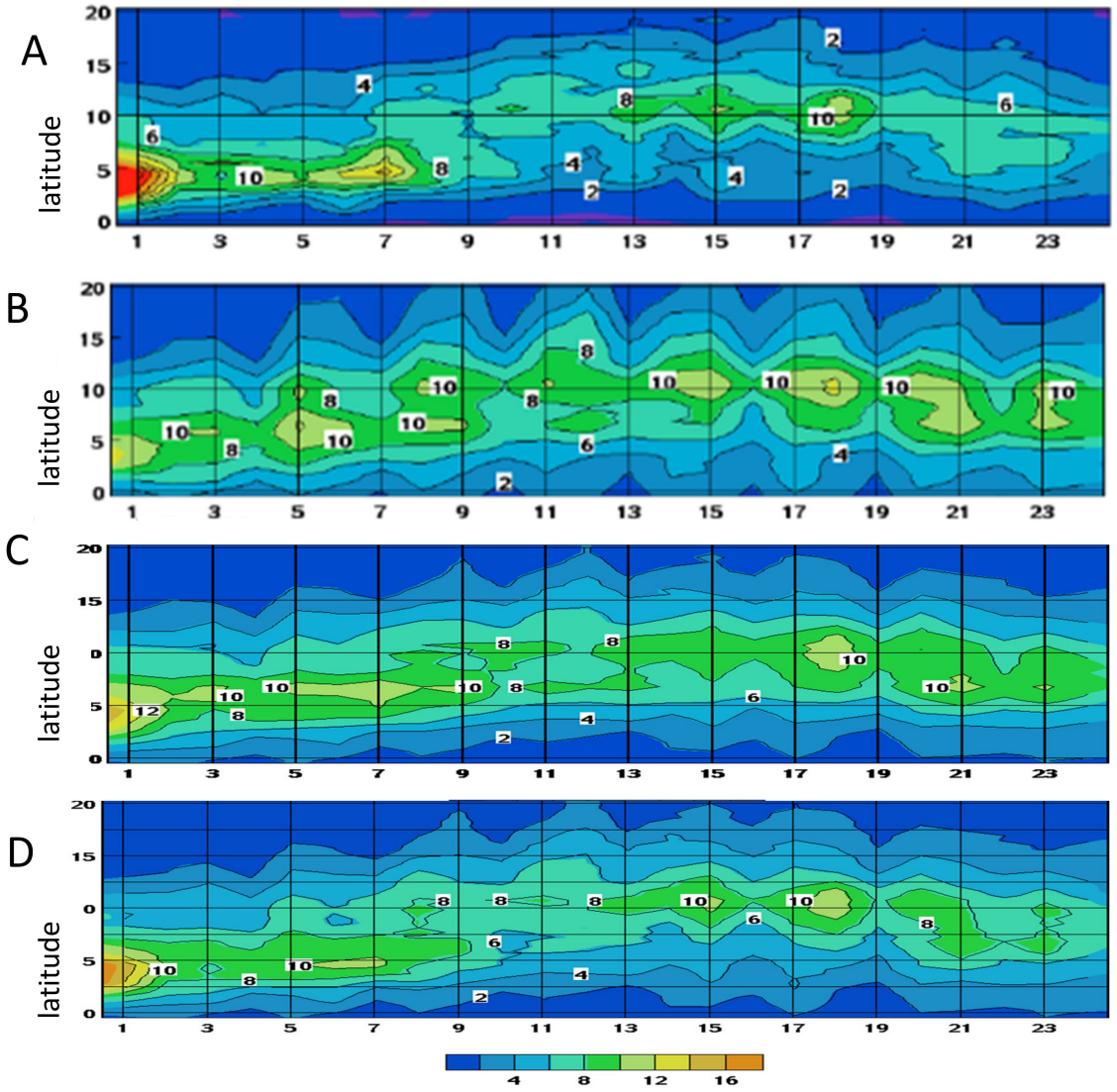

Figure 3. Pentad (5-day mean) precipitation rates (mm day^{-1}) from June–September versus latitude (Hovmöller), averaged over 10° W to 10° E and 1998–2002. Pentad 1 is the 1–5 June mean. (**A**) TRMM; (**B**) RM3nc forced by ModelE without bias corrections; (**C**) RM3bc forced by ModelE with bias corrections to LBCs and SST; (**D**) RM3sst forced by ModelE with bias corrections to only SST.

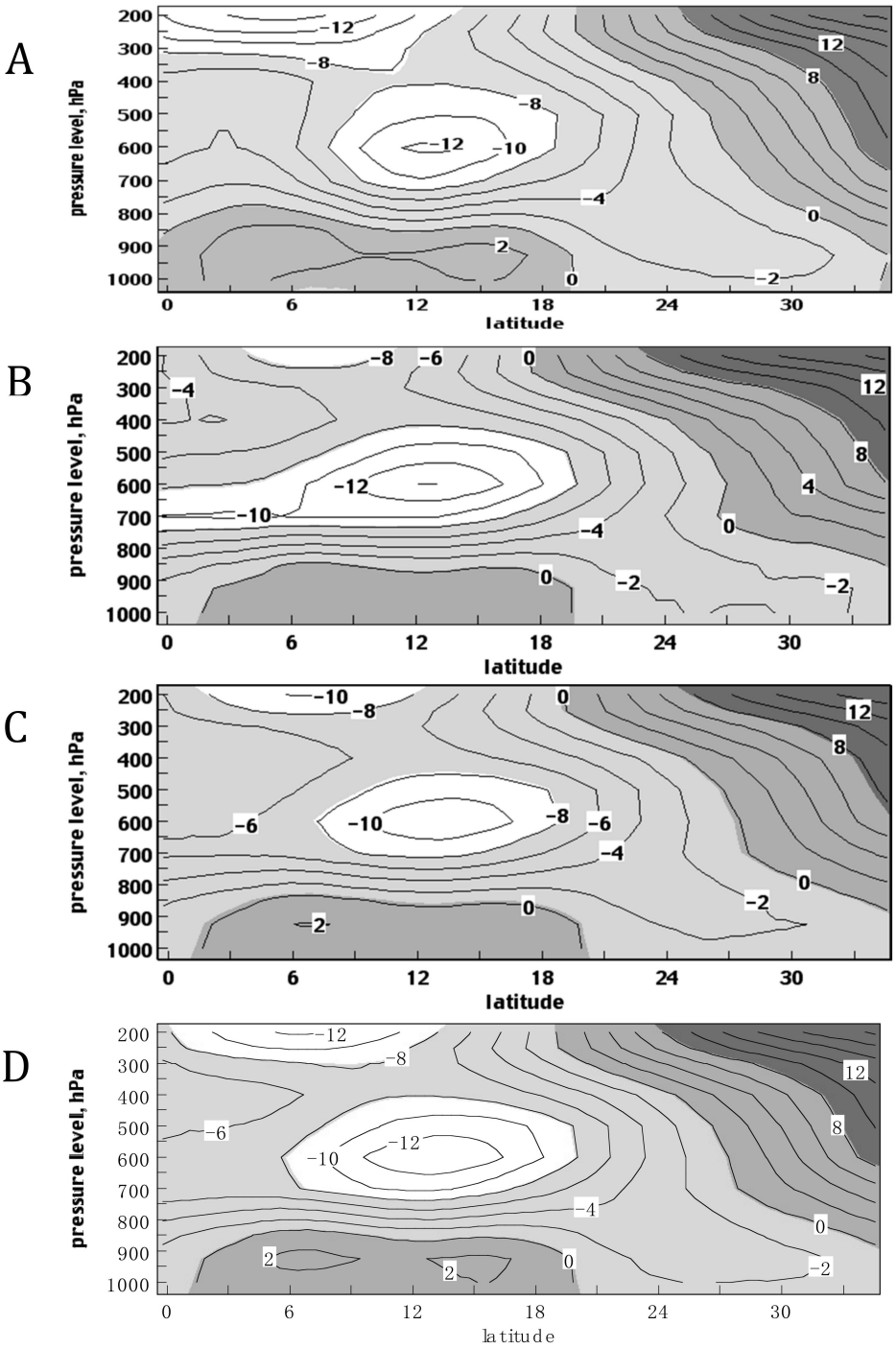

Figure 4. Zonal circulation (m s^{-1}) for June–September 1998–2002, averaged over 10° W to 10° E. (**A**) European Centre for Medium-Range Weather Forecasts Interim reanalysis (ERA-I); (**B**) RM3nc forced by ModelE without bias corrections; (**C**) RM3bc forced by ModelE with bias corrections to LBCs and SST; (**D**) RM3sst forced by ModelE with bias corrections to only SST.

5. Conclusions

The AOGCM-simulated summer monsoon precipitation patterns on a 2° by 2.5° horizontal grid over Africa and the adjacent Atlantic were improved by nesting the RM3 at a 0.44° horizontal resolution. The study is based on data from the 1998–2002 test period, which was shown to have approximately the same mean climate as 1979–2008. However, large biases in AOGCM SST degraded the improvements. This study shows that correcting these SST biases in the regional model's lower boundary conditions

make notable improvements in the RM3-simulated JJAS precipitation accumulations, the seasonal march of the WA precipitation maximum, and the WA zonal wind structure. The RM3 simulation of monsoon onset, missing in the ModelE results, is most impressive. Based on these experiments, however, additionally correcting the LBC biases in the ModelE atmospheric data used to drive the RM3 does not contribute to more realistic simulations of the summer monsoon season over West Africa, and, in some respects, even degrades results. The study suggests that GISS ModelE projections of decadal climate change should benefit from dynamic downscaling with an RCM with demonstrated skill in simulating African climate, using bias-corrected SSTs for lower boundary conditions.

Author Contributions: M.F. had responsibility for all data handling, including input for and output from all simulations and reanalysis fields. L.D. conceived of the study, drafted all figures and wrote the paper.

Funding: This research received no external funding.

Acknowledgments: The authors acknowledge their access to research facilities at NASA/GISS.

Conflicts of Interest: The authors declare no conflict of interest.

References

1. Thorncroft, C.; Nguyen, H.; Zhang, C.; Peyrillé, P. Annual cycle of the West African monsoon: Regional circulations and associated water vapour transport. *Q. J. R. Meteorol. Soc.* **2011**, *137*, 129–147. [CrossRef]
2. Gu, G.; Adler, R. Seasonal evolution and variability associated with the West African monsoon system. *J. Clim.* **2004**, *17*, 3364–3377. [CrossRef]
3. Mohino, E.; Janicot, S.; Bader, J. Sahel rainfall and decadal to multi-decadal sea-surface temperature variability. *Clim. Dyn.* **2011**, *37*, 419–440. [CrossRef]
4. Jung, T.; Ferranti, L.; Tompkins, A.M. Response to the summer of 2003 Mediterranean SST anomalies over Europe and Africa. *J. Clim.* **2006**, *19*, 5439–5454. [CrossRef]
5. Rowell, D. The impact of Mediterranean SSTs on the Sahelian rainfall season. *J. Clim.* **2003**, *16*, 849–862. [CrossRef]
6. Druyan, L. Studies of 21st century precipitation trends over West Africa. *Int. J. Clim.* **2011**, *31*, 1415–1424. [CrossRef]
7. Nicholson, S. The West African Sahel: A review of recent studies on the rainfall regime and its interannual variability. *ISRN Meteorol.* **2013**, *2013*, 453521. [CrossRef]
8. Druyan, L.; Fulakeza, M. Downscaling GISS ModelE boreal summer climate over Africa. *Clim. Dyn.* **2016**, *47*, 3499–3515. [CrossRef]
9. Lim, Y.-K.; Stefanova, L.B.; Chan, S.C.; Schubert, S.D.; O'Brien, J.J. High-resolution subtropical summer precipitation derived from dynamical downscaling of the NCEP/DOE reanalysis: How much small-scale information is added by a regional model? *Clim. Dyn.* **2011**, *37*, 1061–1080. [CrossRef]
10. Kanamitsu, M.; Ebisuzaki, W.; Woollen, J.; Yang, S.-K.; Hnilo, J.; Fiorino, M.; Potter, G. NCEP-DEO AMIP-II Reanalysis (R-2). *Bull. Am. Meteorol. Soc.* **2002**, *83*, 1631–1643. [CrossRef]
11. Denis, B.; Laprise, R.; Caya, D.; Cote, J. Downscaling ability of one-way nested regional climate models: The Big-Brother Experiment. *Clim. Dyn.* **2002**, *18*, 627–646.
12. Haensler, A.; Hagemann, S.; Jacob, D. Dynamical downscaling of ERA40 reanalysis data over southern Africa: Added value in the representation of seasonal rainfall characteristics. *Int. J. Clim.* **2011**, *31*, 2338–2349. [CrossRef]
13. Bernstein, L.; Bosch, P.; Canziani, O.; Chen, Z.; Christ, R.; Davidson, O.; Hare, W.; Huq, S.; Karoly, D.; Kattsov, V.; et al. *Climate Change 2007: Synthesis Report, The Intergovernmental Panel on Climate Change*; IPCC: Geneva, Switzerland, 2007; 73p.
14. Druyan, L.; Fulakeza, M. Downscaling reanalysis over continental Africa with a regional model: NCEP versus ERA Interim forcing. *Clim. Res.* **2013**, *56*, 181–196. [CrossRef]
15. Diallo, I.; Sylla, M.; Giorgi, F.; Gaye, A.; Camara, M. Multi-model GCM-RCM ensemble-based projections of temperature and precipitation over West Africa for the early 21st century. *Int. J. Geophys.* **2012**, *2012*, 972896. [CrossRef]

16. Patricola, C.; Cook, K. Northern African climate at the end of the 21st century: An integrated application of regional and global climate models. *Clim. Dyn.* **2010**, *35*, 193–212. [CrossRef]
17. Vigaud, N.; Roucou, P.; Fontaine, B.; Sijikumar, S.; Tyteca, S. WRF/ARPEGE-CILMAT simulated climate trends over West Africa. *Clim. Dyn.* **2011**, *36*, 925–944. [CrossRef]
18. Paeth, H.; Thamm, H.-P. Regional modeling of future African climate north of 15° S including greenhouse warming and land degradation. *Clim. Chang.* **2007**, *83*, 401–427. [CrossRef]
19. Steiner, A.; Pal, J.; Rauscher, S.; Bell, J.; Diffenbaugh, N.; Boone, A.; Sloan, L.; Giorgi, F. Land surface coupling in regional model simulations of the West African monsoon. *Clim. Dyn.* **2009**, *33*, 869–892. [CrossRef]
20. Moufouma-Okia, W.; Rowell, D. Impact of soil moisture initialization and lateral boundary conditions on regional climate model simulations of the West African monsoon. *Clim. Dyn.* **2010**, *35*, 213–229. [CrossRef]
21. Alo, C.; Wang, G. Role of dynamic vegetation in regional climate predictions over West Africa. *Clim. Dyn.* **2010**, *35*, 907–922. [CrossRef]
22. Giannini, A.; Salack, S.; Loudoun, T.; Ali, A.; Gaye, A.; Ndiaye, O. A unifying view of climate change in the Sahel linking inter-seasonal, interannual and long time scales. *Environ. Res. Lett.* **2013**, *8*, 024010. [CrossRef]
23. Sylla, M.; Coppola, E.; Mariotti, L.; Giorgi, F.; Ruti, P.; Dell'Aquilla, A.; Bi, X. Multiyear simulation of the African climate using a regional climate model (RegCM3) with high resolution ERA-interim reanalysis. *Clim. Dyn.* **2010**, *35*, 231–247. [CrossRef]
24. Sylla, M.; Giorgi, F.; Ruti, P.; Calmanti, S.; Dell'Aquila, A. The impact of deep convection on the West African summer monsoon climate: A regional climate model sensitivity study. *Q. J. R. Meteorol. Soc.* **2011**, *137*, 1417–1430. [CrossRef]
25. Jones, C.; Giorgi, F.; Asrar, G. The coordinated regional downscaling experiment: CORDEX, An international downscaling link to CMIP5. *CLIVAR Exch.* **2011**, *16*, 34–39.
26. Hernandez-Diaz, L.; Laprise, R.; Sushama, L.; Martynov, A.; Winger, K.; Dugas, B. Climate simulation over CORDEX Africa domain using the fifth generation Canadian Regional Climate Model (CRCM5). *Clim. Dyn.* **2013**, *40*, 1415–1433. [CrossRef]
27. Nikulin, G.; Jones, C.; Giorgi, F.; Asrar, G.; Büchner, M.; Cerezo-Mota, R.; Christensen, O.; Déqué, M.; Fernandez, J.; Haensler, A.; et al. Precipitation climatology in an ensemble of CORDEX-Africa regional climate simulations. *J. Clim.* **2012**, *25*, 6057–6078. [CrossRef]
28. Adeniyi, M.O.; Dilau, K.A. Assessing the link between Atlantic Niño 1 and drought over West Africa using CORDEX regional climate models. *Theor. Appl. Climatol.* **2018**, *131*, 937–949. [CrossRef]
29. Misra, V.; Kanamitsu, M. Anomaly nesting: A methodology to downscale seasonal climate simulations from AGCMs. *J. Clim.* **2004**, *17*, 3249–3262. [CrossRef]
30. Rojas, M.; Seth, A. Simulation and sensitivity in a nested modeling system for South America. II. GCM boundary forcing. *J. Clim.* **2003**, *16*, 2454–2471. [CrossRef]
31. Aryal, Y.; Zhu, J. On bias correction in drought frequency analysis based on climate models. *Clim. Chang.* **2017**, *140*, 361–374. [CrossRef]
32. Miller, R.L.; Schmidt, G.A.; Nazarenko, L.S.; Tausnev, N.; Bauer, S.E.; DelGenio, A.D.; Kelley, M.; Lo, K.K.; Ruedy, R.; Shindell, D.T.; et al. CMIP5 historical simulations (1850-2012) with GISS ModelE2. *J. Adv. Model. Earth Syst.* **2014**, *6*, 441–478. [CrossRef]
33. Schmidt, G.A.; Ruedy, R.; Hansen, J.E.; Aleinov, I.; Bell, N.; Bauer, M.; Bauer, S.; Cairns, B.; Canuto, V.; Cheng, Y.; et al. Present day atmospheric simulations using GISS ModelE: Comparison to in-situ, satellite and reanalysis data. *J. Clim.* **2006**, *19*, 153–192. [CrossRef]
34. Schmidt, G.A.; Kelley, M.; Nazarenko, L.; Ruedy, R.; Russell, G.L.; Aleinov, I.; Bauer, M.; Bauer, S.E.; Bhat, M.K.; Bleck, R.; et al. Configuration and assessment of the GISS ModelE2 contributions to the CMIP5 archive. *J. Adv. Model. Earth Syst.* **2014**, *6*, 141–184. [CrossRef]
35. Del Genio, A.; Yao, M.-S. Efficient cumulus parameterization for long-term climate studies. The GISS scheme. In *Cumulus Parameterization*; Monograph Series; Emanuel, K., Raymond, D., Eds.; American Meteorological Society: Boston, MA, USA, 1993; Volume 24, pp. 181–184.
36. Del Genio, A.; Yao, M.-S.; Kovari, W.; Lo, K.-W. A prognostic cloud water parameterization for global climate models. *J. Clim.* **1996**, *9*, 270–304. [CrossRef]
37. Kim, Y.; Moorcroft, P.R.; Aleinov, I.; Puma, M.J.; Kiang, N. Variability of phenology and fluxes of water and carbon with observed and simulated soil moisture in the Ent Terrestrial Biosphere Model (Ent TBM version 1.0.1.0.0). *Geosci. Model. Dev.* **2015**, *8*, 3837–3865. [CrossRef]

38. Huffman, G.J.; Bolvin, D.T.; Nelkin, E.J.; Wolff, D.B.; Adler, R.F.; Gu, G.; Hong, Y.; Bowman, K.P.; Stocker, E.F. The TRMM multi-satellite precipitation analysis (TMPA): Quasi-global, multi-year, combined-sensor precipitation estimates at fine scales. *J. Hydrometeorol.* **2007**, *8*, 38–55. [CrossRef]
39. Druyan, L.; Fulakeza, M.; Lonergan, P. Mesoscale analyses of West African summer climate: Focus on wave disturbances. *Clim. Dyn.* **2006**, *27*, 459–481. [CrossRef]
40. Druyan, L.; Fulakeza, M.; Lonergan, P. The impact of vertical resolution on regional model simulation of the West African summer monsoon. *Int. J. Clim.* **2008**, *28*, 1293–1314. [CrossRef]
41. Druyan, L.; Feng, J.; Cook, K.; Xue, Y.; Fulakeza, M.; Hagos, S.; Konare, A.; Moufouma-Okia, W.; Rowell, D.; Vizy, E. The WAMME regional model intercomparison study. *Clim. Dyn.* **2010**, *35*, 175–192. [CrossRef]
42. Druyan, L.; Fulakeza, M. The impact of the Atlantic cold tongue on West African monsoon onset in regional model simulations for 1998–2002. *Int. J. Clim.* **2014**, *35*, 275–287. [CrossRef]